ONLINE FIRST October 10, 2024

Engineering Transactions, **72**, doi: 10.24423/EngTrans.3385.2024
Institute of Fundamental Technological Research Polish Academy of Sciences (IPPT PAN)
Université de Lorraine • Poznan University of Technology

OSA 2024

Active Vibration Control of Pipe-Shaped Robot Arm

Marcin Adam PATER*, Lucyna LENIOWSKA, Marcin GROCHOWINA

Department of Mechatronics and Control Engineering
University of Rzeszow
Rzeszow, Poland

*Corresponding Author e-mail: mpater@ur.edu.pl

Robotic systems, because of their construction, are susceptible to vibrations that significantly affect their accuracy. Consequently, many efforts are made to eliminate vibrations and stabilize the structure as effectively as possible through the use of various solutions. This article presents the results of research on the use of piezoelectric elements- micro fiber composite (MFC) to reduce vibrations in a thin-walled tube, serving as a model of a lightweight robot arm. The aim of the research is to develop an effective method for vibration cancelation of considered arm model. In our approach, MFC elements were used to perform dual roles: as sensors and actuators. The object model was obtained based on measurements taken on a laboratory stand using an acquisition card and the xPC Target (Matlab) environment. Based on the obtained data, an ARX-type model was developed, and an optimal controller was selected for application in the designed active vibration reduction system. The article includes the results of tests carried out for several different vibration-inducing signals, confirming the effectiveness of the applied vibration-reduction method.

Keywords: active vibration suppression; parametric identification; ARX model; smart materials; MFC.

1. Introduction

Today, many industries use lightweight robots (LWRs), designed especially for mobility and interaction with unknown environments Fig. 1. They are mainly implemented in applications that require direct interaction with humans.

In contrast to the design of traditional industrial robots, which have very stiff arms and inherently heavy manipulators, LWRs are modeled after human arms. This design offers several advantages, including ease of adaptation to new environments and compliance with relevant safety standards. On the other hand, due to their lightweight design and high load-to-weight ratio, LWRs are more prone to unwanted vibrations compared to standard industrial robots [16]. This

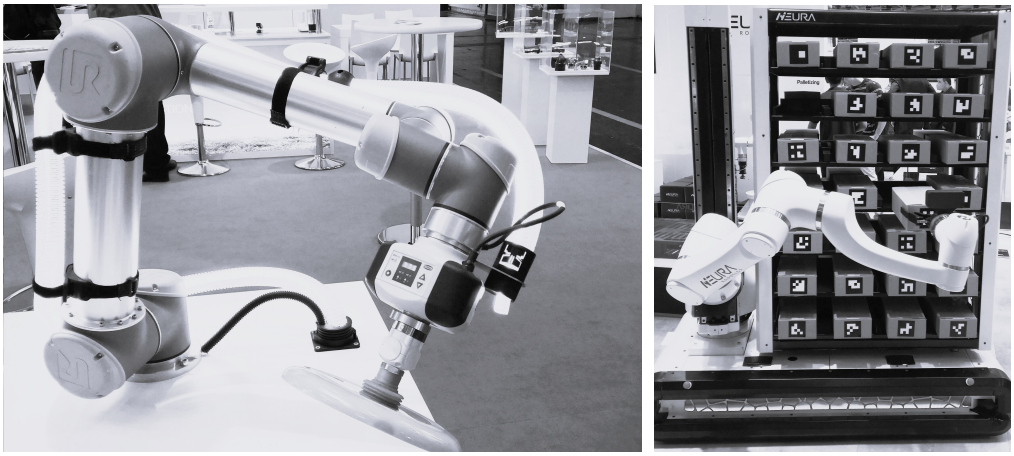

FIG. 1. Examples of lightweight robots (LWRs) (photo by L. Leniowska).

feature has a significant effect on the robot's accuracy. In such circumstances, measuring the end-point position and orientation for feedback can be a challenging task. Moreover, the built-in LWR motors usually cannot respond in time to match the frequency range of the end-point vibrations.

Over the years, most researchers have addressed this problem by incorporating the flexibility of the LWR into controller design. They have proposed increasingly advanced control algorithms, such as integer and fractional order proportional-integral-derivative (PID) control [2, 17], sliding mode control [18, 19], and predictive control. Additionally, methods such as pole assignment schemes, linear quadratic Gaussian (LQG), and the optimal control algorithm (LQR) have also been applied to various structures by researchers [4, 6, 8].

In recent years, some studies on active vibration suppression have provided new, effective technical approaches. Vibration can be effectively reduced by adding special damping coatings or damping paths distributed along the structure, which have a little influence on the weight of the pipe-shaped arm. Therefore, the desired stiffness of the structure can be improved, efficiently reducing the flexibility that degrades the closed-loop performance of LWRS. Moreover, this method allows for the reduction of LWR arm flexibility independently on the robot's motion trajectory design. The use of this solution remarkably simplifies both design of robot trajectory motion and controller design. This approach, known as the 'segment controller' method for shaping local three-dimensional deformation, was designed and presented in [9]. However, this is a very demanding solution, as the control system has a multi-segment chain structure that requires multichannel, two-way communication with synchronization. It is therefore very difficult to implement it on miniature ARM processors.

In order to compensate the effects of the inherent elasticity of the robot arm caused by vibrations, a more traditional feedback-based active vibration control method has been chosen. This approach is widely applied in piezoelectric structural vibration suppression. This method has been used successfully to reduce vibrations in planar structures, such as circular and trapezoidal plates [5, 8, 12].

In the context of LWR robot design, strong emphasis is placed on selecting materials for the robotic structure. Ideal materials are those that combine lightness and strength, such as aluminum alloys, titanium alloys, or carbon fibers. This article presents research results on the use of piezoelectric elements (MFC) to reduce vibrations in a thin-walled pipe made of aluminum alloy, serving as a model for a lightweight robot arm (Fig. 2).

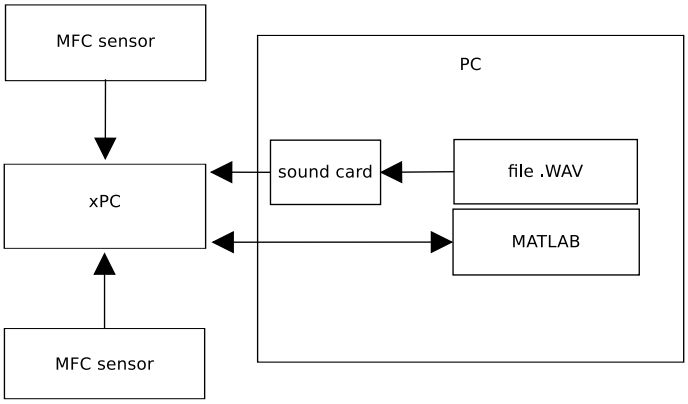

FIG. 2. Block diagram of the measurement system.

In this research, special attention is given to MFC elements, due to their thin, flexible sheet construction, which allows them to be implemented as both sensors and bending actuators, providing significant structural deflection. There are many works that aimed to study piezoelectric applications, see [5, 7, 13].

The aim of this paper is to present an effective method for vibration cancelation of the considered robot arm model, which is pipe-shaped. In the research, we use an active method to reduce vibrations in a flexible robot arm in such a way that the damping algorithms do not place a burden on the robot's joints. This approach improves the desired stiffness of the structure, effectively blocking its flexibility, which usually impairs the performance of LWRs.

The vibration characteristics of pipes are complex and exhibit rich nonlinear dynamic phenomena; therefore, it is difficult to develop an accurate vibration model using analytical theory. Therefore, the object model used here was obtained through a parametric identification method [10], which relied on mea-

surements taken on a laboratory stand. Vibration measurements were recorded using an acquisition card and the xPC Target environment (Matlab) [11]. Based on the obtained data, an ARX-type object model was developed, and a PID-type controller was selected and applied in the designed active vibration reduction system. The results of tests conducted with various vibration-inducing signals, including sinusoidal vibrations at the object's resonant frequency and interference in the form of soft noise and chirping, confirm the effectiveness of the designed controller. Simulation results showed that for the considered object, the applied PID-type controller achieved very promising significant vibration reduction. For optimal results of LWRs, this approach can be applied in a cascade controller configuration (with a PID vibration suppression controller as the slave and a position/orientation motion controller in the robot joints as the master).

2. Construction of the test stand

The test stand was built based on the xPC Target module of the MATLAB package and MFC elements (Table 1). The control object was an aluminum pipe made of Al99.5 aluminum alloy, with a diameter of $\phi = 38$ mm, a wall thickness $d = 2$ mm and a length $l = 2000$ mm. A block diagram of the data flow at the station is shown in Fig. 2, and a schematic of the considered object with the arrangement of MFC elements is shown in Fig. 3. During the experiment, the MFCs served as sensors, actuators and exciters.

Table 1. MFC parameters.

Dimension	06L18-044D	11D18026D
Width [mm]	34	34
Height [mm]	103	67
Depth [mm]	0.3	0.3
DC poling voltage, Vpol [V]	1500	±1500
d31 [pm/V]	−2.1E+02	−2.1E+02
d33 [pm/V]	4.6E+02	4.6E+02

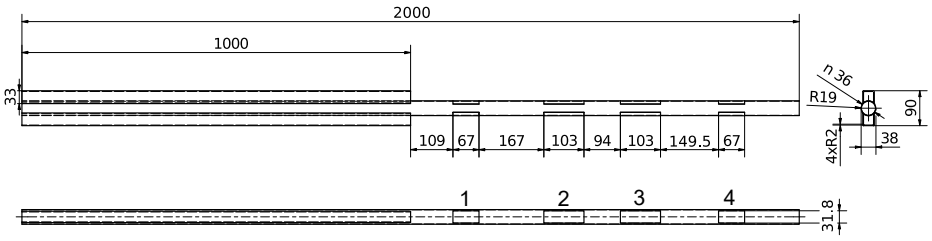

Fig. 3. Schematic oof MFC element arrangement: 1, 2, 4 – sensors, 3 – actuator.

MFCs are advanced piezoelectric materials that consists of long piezoelectric fibers fused into a polymer composite. This structure allows for better adaptability and flexibility compared to traditional piezoelectric materials. MFCs can generate an electric charge in response to mechanical stress, and conversely, they deform when an electric voltage is applied. Moreover, MFCs are characterized by their small size and lightweight design, low power consumption, fast response times, and ability to easily integrate with the structure of the control object. For these reasons, they are particularly useful in active vibration control applications, which were used in our tests.

In order to select optimal mounting locations for the piezoelectric elements, a Polytec vibrometer was used to determine areas of highest activity in the object during its excitation. The object was subjected to vibrations using a chirp signal ranging from 1 Hz to 1 kHz over a duration of 30 seconds.

The MFCs were mounted in pairs – one on the upper side of the object and the other on the lower side. A total of three pairs of MFC transducers were installed. Their schematic arrangement is shown in Fig. 3, and the tested object with the installed transducers is depicted in Fig. 4.

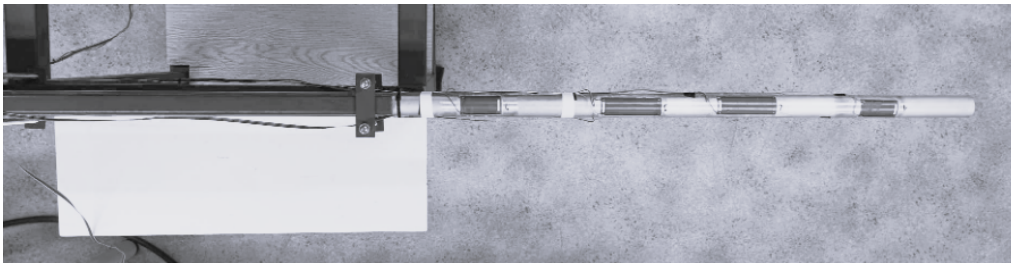

Fig. 4. Tested object with MFC elements attached.

The xPC Target module, also known as Simulink Real Time, is a MATLAB tool for rapid prototyping, testing and implementation of control systems in real time. It supports software-hardware communication. Thanks to this module, it is possible to connect to control and measurement cards. The xPC Target module enables real-time data collection, which is necessary for the analysis and optimization of the control system [1, 11]. In the experiment, 8SE SSH A/D PCI multifunction board was used.

3. System model

It is well known that most control law design methods require an explicit mathematical model of the system to be controlled. A suitable model must have the right balance between complexity and sufficient accuracy. The structure un-

der study is a vibrating tube with a radius $a = 30$ mm, clamped on one side, as shown in Fig. 4. MFC elements were glued to the upper and lower surfaces of the tube. The locations of the MFC elements were determined experimentally using a laser vibrometer. The derivation of models for the structures in question can be carried out in two ways. The first method involves modeling the structural dynamics using partial differential equations derived from physical principles. The second method, commonly known as black-box modeling or system identification [10, 15], allows for the inference of a model from a set of data collected during practical experiments. In the identification process, a parametric model of the system is determined based on the recorded input and output data. Analog signals measured by the sensors are amplified and converted into digital form. The next step is data preprocessing. It can be done by using a digital filter that eliminates DC components and high-frequency noise. We assume that the sampled signal values can be related through the linear difference equation given by Eq. (3.1) [10]:

$$y(k) + a_1 y(k-1) + ... + a_{n_A} y(k-n_A) = b_1 u(k-d) + ... + b_{n_B} u(k-d-n_B+1) + n(k), \tag{3.1}$$

where $y(k)$, $u(k)$ represents, respectively, the output and input in discrete time $k = 1, 2, 3, ..., n_A$ is the number of poles, n_B is the number of zeros, d is the number of samples before the input affects the output of the system, and $\eta(k)$ denotes some disturbance of unknown character. The relationship shown above, known as an autoregressive model with exogenous input (ARX), can be rewritten as [3]:

$$A(z^{-1})y(k) = B(z^{-1})u(k-d) - \eta(k), \tag{3.2}$$

where $A(z^{-1})$ and $B(z^{-1})$ are polynomials in the delay z^{-1} operator:

$$A(z^{-1}) = 1 + a1z^{-1} + ... + a_{n_A} z^{-n_A}, \tag{3.3}$$

$$B(z^{-1}) = b_1 + b_2 z^{-1} + ... + b_{n_B} z^{-n_B+1}. \tag{3.4}$$

Typically, for the mathematical description of the object model, the controller uses transfer functions, in which the coefficients of the polynomials in the numerator and denominator dictate the dynamics. The polynomials $A(z^{-1})$ and $B(z^{-1})$ correspond to the discrete transmittance of the object, which can be determined based on of data collected during practical experiments. Below is a block diagram for closed-loop control system with the designed PID-type controller. In the block diagram (Fig. 5), the $R(z^{-1})$ and $S(z^{-1})$ represent the polynomials in the discrete controller's transmittance, the coefficients of which

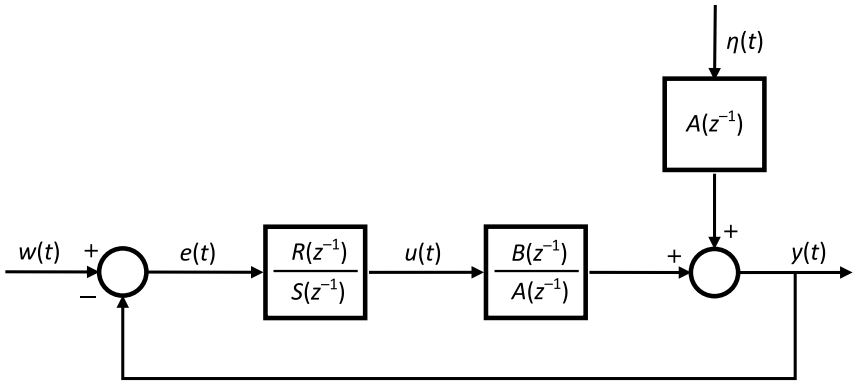

FIG. 5. Diagram of the considered closed-loop system.

should be calculated and will be determined for vibration cancellation based on classic PID rules or determined using the pole placement method. The high sampling rate applied in the tests, which is significantly greater than the highest measured frequency, allows us to approximate the system as continuous despite the discrete nature of the measurements.

4. Object identification

First, the object was identified in order to determine its transmittance. Tests were performed at sampling rates of 2000 S/s, 5000 S/s and 10 000 S/s, with the amplitude of the forcing signal fed to the MFC set to 600 Vpp. Measurements were carried out in parallel from three MFC sensors in order to select the best data for creating the object model. The object was excited with a chirp signal ranging from 1 Hz to 1 kHz. The signal was generated with Audacity software using the "generate chirp" function. The sampling rate was set at 44 100 S/s with a resolution of 16 bit. Forcing duration was set to 30 seconds, supplemented by 5 seconds of silence before and after the chirp signal. The WAV format was used to record the forced signal to avoid loss of quality in the sound file. The computer's sound card [14] was used as the signal source. The signal was sent to the measurement card and to the amplifier connected to the MFC. A Polytec laser vibrometer was used to measure the vibration amplitude independently of the control system. The setup of the measurement station is shown in Fig. 6.

The identification process involves fitting a mathematical model to a set of experimental data. For this purpose, two main signals were necessary: the excitation signal, i.e., the chirp, which was responsible for stimulating the system, and the object response signal, which was recorded using the selected MFC sen-

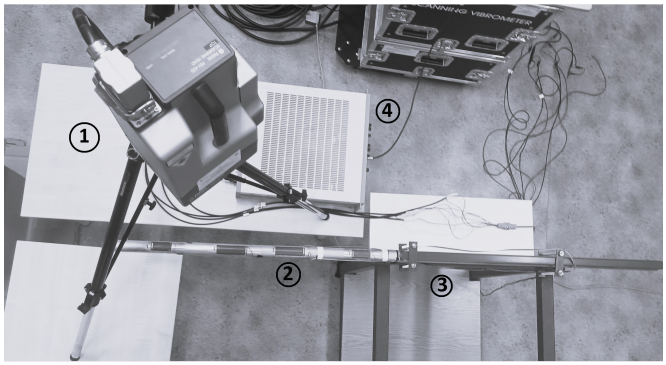

FIG. 6. Measurement station setup: 1 – vibrometer measuring head, 2 – tested object with MFC elements attached, 3 – mounting for the tested object, 4 – amplifier for MFC elements.

sor. Identification was performed using the Ident module of MATLAB, and the results are presented in Fig. 7. The accuracy of the derived model was estimated according to the criterion of the least squares Method, the most commonly used technique as long as the fitting function is a polynomial.

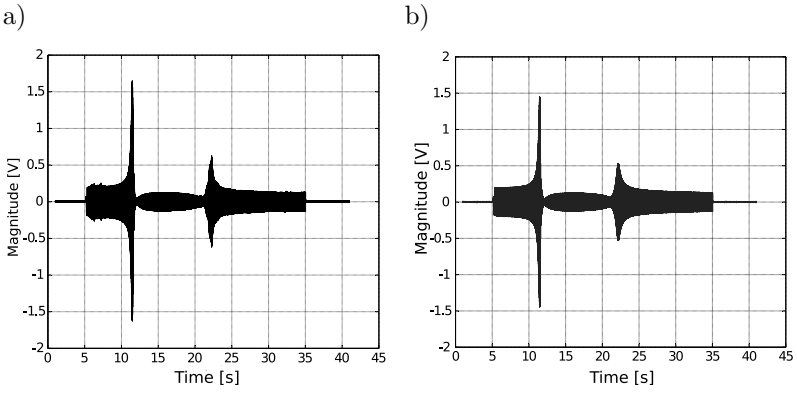

FIG. 7. Measured and simulated model output:
a) measured object response, b) obtained object model response.

The object model that, with the assumed accuracy, is closest to the real data has the form [3]:

(4.1)
$$G(z^{-1}) = \frac{b_0+b_1z^{-1}+b_2z^{-2}+b_3z^{-3}+b_4z^{-4}+b_5z^{-5}+b_6z^{-6}}{a_0+a_1z^{-1}+a_2z^{-2}+a_3z^{-3}+a_4z^{-4}+a_5z^{-5}+a_6z^{-6}+a_7z^{-7}+a_8z^{-8}},$$

where the coefficients a_i and b_i take the values listed in Table 2.

Table 2. Values of the polynomials coefficients $A(z^{-1})$ and $B(z^{-1})$ used in the model fitting process.

i	$A(z^{-1})$	$B(z^{-1})$
8	−0.1884	
7	−2.6302	
6	3.6603	0.1884
5	0.3622	0.9186
4	−4.5864	−1.8171
3	1.4705	1.8222
2	3.8575	−0.9263
1	−3.7037	0.1909
0	1	0

4.1. Controller design

In the considered configuration of the control system, a commonly used PID controller was applied. The settings were selected using the MATLAB toolbox [3].

A series of tests were performed for the step functions and for sinusoidal signals. The purpose of these tests was to assess the behavior of the system with the PID controller used in various operating conditions and to check whether the obtained controller parameters ensure appropriate system operation for various types of input signals.

The PID controller setting values used in the simulations are listed in Table 3.

Table 3. PID controller settings for simulations.

Proportional (P)	7.1
Integral (I)	0.6
Derivative (D)	−4.4

4.2. Results of simulation

To carry out the simulation process, it was necessary to determine the resonance frequencies of the object using its response. Two resonance frequencies were determined: 214 Hz and 574 Hz (Fig. 8).

The next step involved building a simulation model that would allow to control system to be activated after a given time. Simulations were performed for sinusoidally variable signals. The signals used for the excitation were:

- sinusoidal signal with a frequency of 214 Hz,
- sinusoidal signal with a frequency of 574 Hz,
- sum of signals at resonant frequencies,
- chirp signal ranging from 1 Hz to 1 kHz,
- white noise.

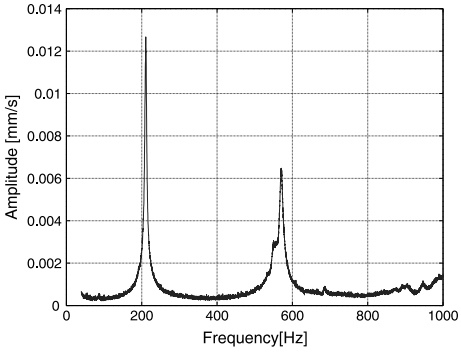

FIG. 8. Frequency characteristics of the tested object.

The simulation time for each excitation signal was 40 seconds. The controller was turned off for the first 20 seconds and was turned on at the 20th second of the simulation. The chirp signal was generated twice within the 40 seconds, in batches of 20 seconds each. Graphs presenting the simulation result are shown in Figs. 9–13.

Figures 9–11 show the response of the object under excitation corresponding to the first and second harmonic modes, as well as their combined affect. It can

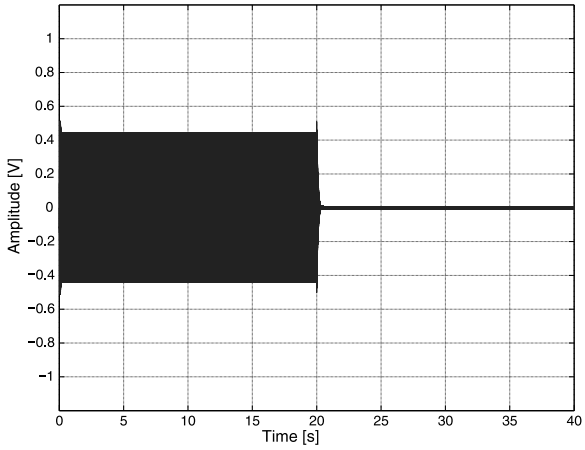

FIG. 9. Response of the object to a 214 Hz sinusoidal excitation signal; 0–20 s indicates the open-loop control system, 20–40 s indicated the closed-loop control system.

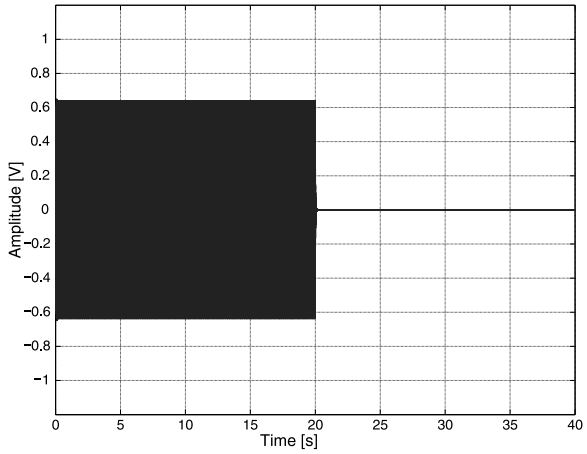

FIG. 10. Response of the object to a 574 Hz sinusoidal excitation signal; 0–20 s indicates the open-loop control system, 20–40 s indicates the closed-loop control system.

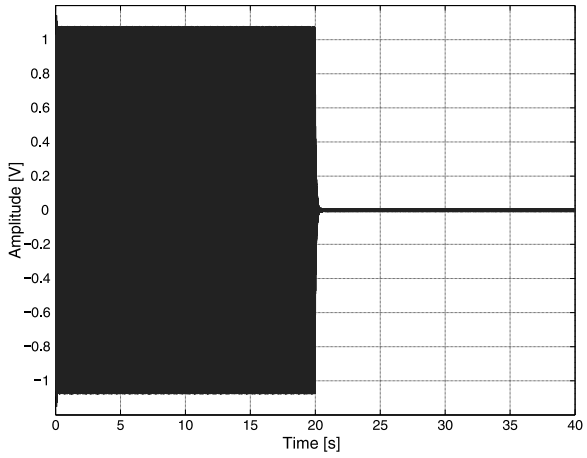

FIG. 11. The object response to the excitation caused by the sum of first two resonant frequencies; 0–20 s represents the open-loop control system, 20–40 s indicated the closed-loop control system.

be seen that the designed controller, which was activated after 20 seconds very effectively reduces the vibrations of the object. In Figs. 12 and 13, excitation not related to the natural frequencies of the object was used. As can be seen here, the designed controller also very effectively reduces the vibrations of the arm.

Finally, it can be stated that a high level of vibration reduction was achieved for each tested excitation signal. Both the individual resonance frequencies and their combined effect were nearly eliminated in the tested system. Furthermore, non-resonant frequencies also experienced significant attenuation, as can be in-

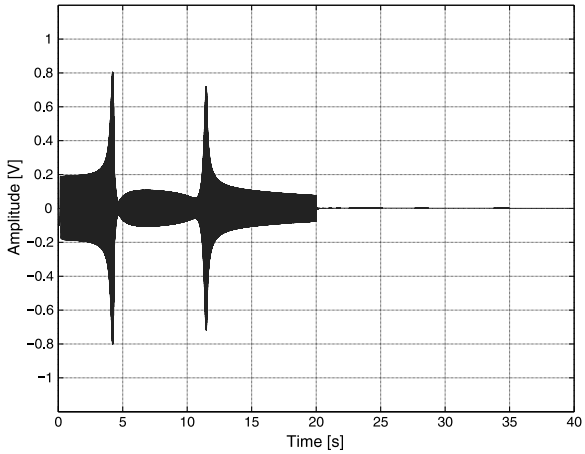

FIG. 12. The object response to a chirp excitation ranging from 1 Hz to 1 kHz, where each chirp signal lasts for 20 s; 0–20 s shows the open-loop control system, 20–40 s demonstrates closed-loop control system.

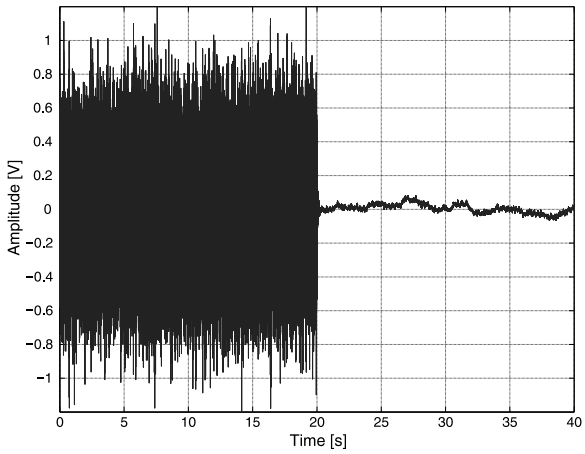

FIG. 13. The object response to white noise excitation; 0–20 s reflects the open-loop control system, 20–40 s represents the closed-loop control system.

ferred from the response to chirp stimulation (Fig. 12) and random noise stimulation (Fig. 13). Based on the conducted research, it can be concluded that the designed regulation system can be used in further empirical research.

5. Summary and conclusions

The aim of this work was to investigate the feasibility of using MFC sensors and actuators to suppress vibrations in an aluminum pipe serving as lightweight

robotic arm. The object model was obtained with the use of parametric identification within the Matlab environment. The placement of the MFC sensors and actuators was determined with the use of a laser vibrometer. For vibration cancelation in the, an effective PID-type controller was designed. To assess the level of vibration reduction, simulation tests were performed for various types of excitation signals, including periodic signals at resonant frequencies, summed resonant signals, chirp signals, and white noise. In conducted tests, the total simulation time was 40 seconds, with the object operating without control for the first 20 seconds, followed by the controller being switched on. This made it possible to compare and observe controller's impact on vibration cancelation. The simulation results showed that the control system worked as intended, effectively stabilizing the object upon the controller's activation. Ultimately, the simulations revealed that the designed PID controller is very effective, achieving vibration reductions exceeding 95% in all tested cases, which practically eliminated vibrations.

For the best control results in LWRs, a master–slave configuration can be implemented, where a slave controller manages PID vibration suppression, while a position/orientation motion controller operates as the master, localized at the robot joints.

References

1. Arseniev D.G., Overmeyer L., Kälviäinen H., Katalinić B., *Cyber-Physical Systems and Control*, *Lecture Notes in Networks and Systems* (LNNS), Vol. 95, Springer Nature, 2019, doi: 10.1007/978-3-030-34983-7.

2. Birs I., Muresan C., Nascu I., Ionescu C., A survey of recent advances in fractional order control for time delay systems, *IEEE Access*, 7: 30951–30965, 2019, doi: 10.1109/ACCESS.2019.2902567.

3. Isermann R., *Digital Control Systems*, Springer Science & Business Media, 2013.

4. Leniowska L., Modelling and vibration control of planar systems by the use of piezoelectric actuators, *Archives of Acoustics*, **34**(4): 507–519, 2009.

5. Leniowska L., Grochowina M., Sierżęga M., Hołota B., An adaptive method for reducing vibrations of circular plates with recursive identification, *Applied Sciences*, **12**(5): 2723, 2022, doi: 10.3390/app12052723.

6. Leniowska L., Leniowski R., The joint vibration analysis of a multi-link surgical manipulator, *Archives of Acoustics*, **37**(4): 475–482, 2012.

7. Leniowska L., Mazan D., MFC sensors and actuators in active vibration control of the circular plate, *Archives of Acoustics*, **40**(2): 257–265, 2015, doi: 10.1515/aoa-2015-0028.

8. Leniowska L., Sierżęga M., Vibration control of a circular plate using parametric controller with phase shift adjustment, *Mechatronics*, **58**: 39–46, 2019, doi: 10.1016/j.mechatronics.2019.01.003.

9. Leniowski R., Leniowska L., The multi-segment controller of a flexible arm, [in:] *ISR 2020; 52th International Symposium on Robotics*, pp. 71–78, VDE, 2020.

10. Ljung L., *System Identification: Theory for the User*, Prentice Hall PTR, 1999.

11. *MathWorks Documentation, Simulink Real-Time Documentation*, 2023. Available at: https://www.mathworks.com/help/simulink-real-time/, retrieved on: 2024.09.02.

12. Mierzejewski K., Leniowska L., Design of control system for active vibration suppression of trapezoidal plate, *Vibrations in Physical Systems*, **30**(1): 1–8, 2019.

13. Sierżęga M., Leniowska L., The application of xPC Target platform for a circular plate vibration control, *Solid State Phenomena*, **248**: 135–141, 2016, doi: 10.4028/www.scientific.net/ssp.248.135.

14. United Electronic Industries, *500 ks/s, 16-bit, 8SE SSH A/D PCI multifunction board*. Available at: https://www.ueidaq.com/products/500-ks-s-16-bit-8se-ssh-a-d-pci-multifunction-board; retrieved on: 2024.09.02.

15. Van den Bosch P.P.J., Van der Klauw A.C., *Modeling, Identification and Simulation of Dynamical Systems*, CRC Press, 2020.

16. Wang J., Li Y., Hu G., Yang M., Lightweight research in engineering: A review, *Applied Sciences*, **9**(24): 5322, 2019, doi: 10.3390/app9245322.

17. Zhang D., Wei B., A review on model reference adaptive control of robotic manipulators, *Annual Reviews in Control*, **43**: 188–198, 2017, doi: 10.1016/j.arcontrol.2017.02.002.

18. Zhou M., Su H., Feng Y., Wei K., Xu W., Cheng J., Super-twisting algorithm-based fractional-order sliding-mode control of nonlinear systems with mismatched uncertainties, *IEEE Transactions on Industrial Electronics*, **71**(8): 9510–9519, 2024, doi: 10.1109/TIE.2023.3329164.

19. Zhou W., Wang Y., Liang Y., Sliding mode control for networked control systems: A brief survey, *ISA Transactions*, **124**: 249–259, 2022, doi: 10.1016/j.isatra.2020.12.049.

Received July 22, 2024; accepted version September 22, 2024.
Online first October 10, 2024.